A Spectroscopic Investigation of Donor-Acceptor-Substituted Heptalenes

by **Philipp Ott** and **Hans-Jürgen Hansen***

Organisch-chemisches Institut der Universität Zürich, Winterthurerstrasse 190, CH-8057 Zürich

Dedicated to *André M. Braun* on the occasion of his 60th birthday

It is shown that the heptalene-4,5-dicarboxylates **5** react with their Me group at C(1) with *N*,*N*-dimethylformamide dimethyl acetal or other acetals of this type in *N*,*N*-dimethylformamide (DMF) to give the corresponding 1-[(*E*)-2-(*N*,*N*-dialkylamino)ethenyl]-substituted heptalene-4,5-dicarboxylates **8a**–**8e** as well as **8k** and **8i** in good yields (*Table 1*). In a similar manner, the 1-[(*E*)-2-pyrrolidinoethenyl]-substituted heptalene-5-carboxylates **8f**–**h** were synthesized from the corresponding heptalene-carboxylates **10**–**12**, carrying a CHO, CN, or (*E*)-2-(methoxycarbonyl)ethenyl group at C(4) (*Table 1*). All new heptalenes with the π-donor and π-acceptor groups at C(1) and C(4), respectively, exhibit a strongly enhanced heptalene band I in the spectral region of 450–500 nm in MeCN (*Table 7* and *Figs. 4–7*), whereby the specific position is dependent on the π-donor quality of the *N*,*N*-dialkylamino substituent at C(2′) and the π-acceptor property of the group at C(4). The position of heptalene band I is also strongly solvent-dependent as is demonstrated in the case of heptalene **8i** (*Table 9*). A good linear correlation with the CT band of 1-(diethylamino)-4-nitrobenzene or (*E*)-4-(dimethylamino)-β-nitrostyrene (*Figs. 11* and *12*) characterizes the heptalene band I also as an electronic CT transition. Irradiation into this band of **8i** leads, as observed in other cases (*cf.* [1]), to a double-bond shift in the heptalene moiety (→ **8′i**; *Figs. 8–10*). On warming in solution, **8′i** is converted quantitatively to **8i**.

1. Introduction. – Recently, we have demonstrated that suitably di-π-substituted heptalenes, which generally exist in two thermally or photochemically interconvertible double-bond-shifted (DBS) isomers, *i.e.*, π-bonding states, may principally act as π-switches due to the different UV/VIS absorption behavior of the two isomers [1]. An example is displayed in *Fig. 1*. The donor-acceptor-substituted heptalene-5-carboxylate **1**, which carries the donor and the acceptor substituent in conjugative interaction *via* the peripheral heptalene subunit C(1)–C(4), exhibits in the long-wavelength region, at 440 nm, a strong absorption band, in contrast to its DBS isomer **1′** with interrupted direct conjugation *via* the heptalene subunit C(1)–C(4), giving rise to only a very weak absorption band at 440 nm [1b].

Since the starting material for heptalenes of type **1** are corresponding dimethyl heptalene-4,5-dicarboxylates carrying a Me substituent at C(1), which are converted in several steps into **1** and analogs of it (*cf.* [1]), we were interested in a simpler synthesis of donor-acceptor-substituted heptalenes from their dicarboxylate progenitors, so that the MeOCO group at C(4) could act already as π-acceptor group, and only Me–C(1) had to be changed into a strong π-donating group. In this way, we hoped to get access to a number of structurally systematically varied di-π-substituted heptalenes for a detailed study of donor-acceptor effects across the heptalene π-core.

Meerwein et al. [2] and, later, *Bredereck et al.* [3] have shown that CH-acidic compounds form, on heating with formamide acetals or formamide aminals, enamines,

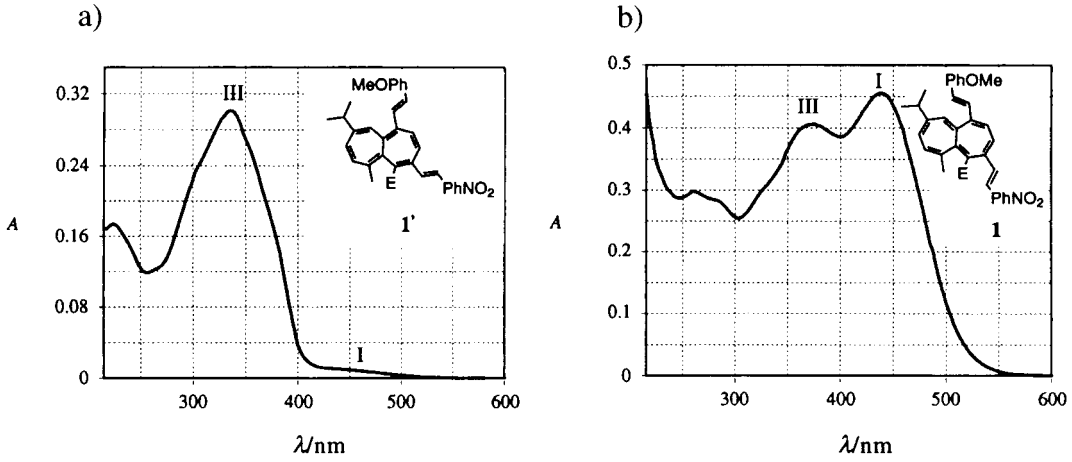

Fig. 1. *UV/VIS Spectra of methyl 9-isopropyl-1-[(*E*)-2-(4-methoxyphenyl)ethenyl]-6-methyl-4-[(*E*)-2-(4-nitrophenyl)ethenyl]heptalene-5-carboxylate* (**1**) *and its DBS isomer* **1'** *in hexane/CH_2Cl_2 9:1* [1c]

and, in 1971, *Leimgruber* and *Batcho* [4] reported on a new and simple indole synthesis – conventionally known today as *Leimgruber-Batcho* indole synthesis (*cf.* [5]) – whereby *o*-nitrotoluenes **2** are treated with dimethylformamide dimethyl acetal (DMFDMA) in dimethylformamide (DMF) at or close to reflux temperature, leading in excellent yields to the formation of the corresponding 1-[2-(dimethylamino)ethenyl]-2-nitrobenzenes **3** (*Scheme 1*). Reductive ring closure of **3** gives then the indole derivatives **4** [4]. Our experience with the reactivity of Me–C(1) of dimethyl 9-isopropyl-1,6-dimethyl- (**5a**) or 1,6,8,10-tetramethylheptalene-4,5-dicarboxylate (**5b**), and their analogs had taught us that deprotonation reactions, followed by addition of electrophiles, are possible (*Scheme 2*). We wondered, therefore, whether the first step of the *Leimgruber-Batcho* procedure would also be applicable to **5a** and its analogs. Indeed, Me–C(1), which stands in conjugative interaction with E_{Me}–C(4), can be functionalized with *N,N*-disubstituted formamide dimethyl acetals **9** to give the corresponding 1-(2-aminoethenyl)-substituted heptalene-4,5-dicarboxylates **8**. We report here on the different donor-acceptor-substituted heptalene-5-carboxylates obtained by this procedure.

Scheme 1

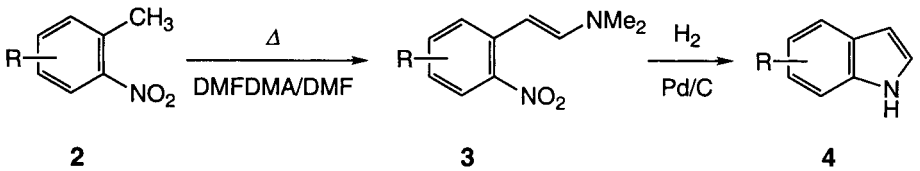

2. Syntheses of Donor-Acceptor-Substituted Heptalene-5-carboxylates. – Reaction of the heptalene-4,5-dicarboxylates **5** with commercially available DMFDMA (**9a**) in DMF at 110°/19 h gave the corresponding enamine **8a** in 71% yield. All the other

Scheme 2

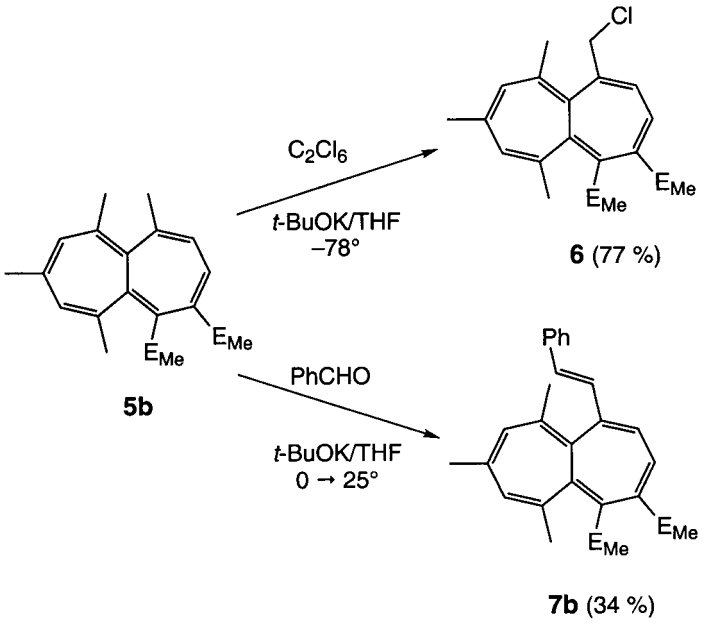

enamines **8b**–**8i**, which are presented in *Table 1*, were prepared by preceding transamination of DMFDMA with the corresponding secondary amines in DMF. The realized yields indicate that basic amines such as Me_2NH, pyrrolidine, and piperidine, as well as an E_{Me} or CN group at C(4), favor the enamine formation. On the other hand, less basic amines such as morpholine or azetidine or a CHO group instead of E_{Me} at C(4) give low yields of the enamine-forming reaction. Moreover, the enamine **8b**, derived from azetidine, turned out to be extremely sensitive to hydrolysis. Therefore, it might be that the low yield of **8b** is partly due to decomposition during the workup procedure. As a rule, all enamines could easily be hydrolyzed; *e.g.*, enamine **8a** was transformed into aldehyde **13** in almost quantitative yield, when treated in THF/H_2O at ambient temperature for 5 h with a catalytic amount of AcOH (*Scheme 3*).

Scheme 3

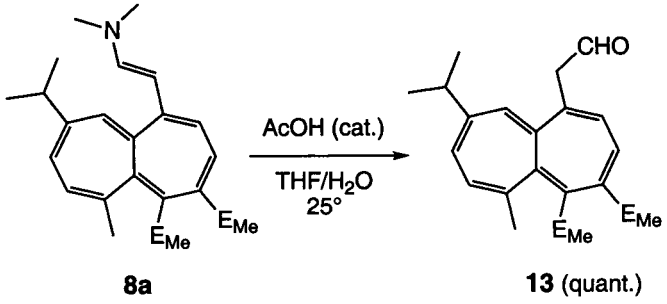

Table 1. *Reaction of 1-Me-Substituted Heptalene-5-carboxylates* **5** *Carrying an Acceptor Group at C(4) with Formamide Dimethyl Acetals*

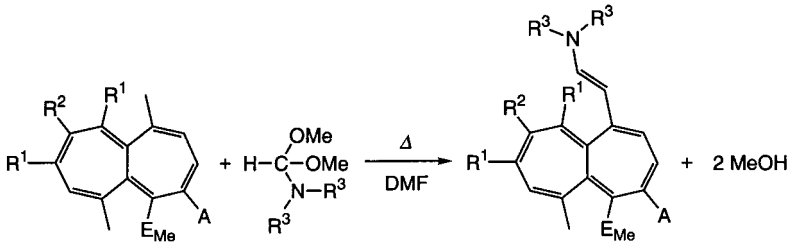

5,10–12 **9** **8**

Entry		Heptalene-5-carboxylate			Amide Acetal		Temp. [°]	Time [h]	Enamine	
	A	R^1	R^2	No.	R^3	No.			No.	Yield [%]
1	E_{Me}	H	i-Pr	**5a**	Me	**9a**	110	3	**8a**	71
2	E_{Me}	H	i-Pr	**5a**	$-(CH_2)_3-$	**9b**	70	6	**8b**	11
3	E_{Me}	H	i-Pr	**5a**	$-(CH_2)_4-$	**9c**	110	3.5	**8c**	95
4	E_{Me}	H	i-Pr	**5a**	$-(CH_2)_5-$	**9d**	110	3.5	**8d**	60
5	E_{Me}	H	i-Pr	**5a**	$-(Ch_2)_4O-$	**9e**	110	10	**8e**	16
6	CHO[a])	H	i-Pr	**10**	$-(CH_2)_4-$	**9c**	110	3	**8f**	10
7	CN[b])	H	i-Pr	**11**	$-(CH_2)_4-$	**9c**	110	1.5	**8g**	97
8	$CH{=}CHE_{Me}$[c])	H	i-Pr	**12**	$-(CH_2)_4-$	**9c**	50	3.5	**8h**	33
9	E_{Me}	Me	H	**5b**	$-(CH_2)_4-$	**9c**	110	1	**8i**	90
10	E_{Me}	Me	H	**5b**	Me	**9a**	110	6	**8k**	75

[a]) The formyl-ester **10** was prepared as described in [1] (see also [7]). [b]) The cyano-ester **11** was prepared from **10** *via* the oxime (see *Exper. Part*). [c]) The (*E*)-configured, vinylic diester **12** was prepared from **10** by a *Wittig* reaction (see *Exper. Part*).

We were quite surprised to notice that a vinylic E_{Me} group at C(4) still induced the enamine formation with an acceptable yield (see *Entry 8* in *Table 1*).

Most of the new heptalenes **8** with the (*E*)-(2-aminoethenyl) group at C(1) crystallized well in brick-to-bordeaux-red crystals (see later). Heptalenes **8a**–**8f** showed in solution no tendency to form their DBS isomers **8′a**–**8′f** on heating or irradiation, as we have observed already with **5a** itself (*cf.* [8]) or other derivatives of it (*cf.* [1]). The amount of the DBS isomers in thermal equilibrium at ambient temperature must, therefore, be well below 1%. Nevertheless, first flash-irradiation experiments with **5a** and its derivatives at ambient temperature demonstrate that they are photochemically switchable, but revert according to the low energy barrier, which separates the '1,2-forms' from their '4,5-forms', very fast to the thermodynamically much more stable '4,5-forms'[1]). Since heptalenes and their DBS isomers with substituents in all four *peri*-positions are separated by higher energy barriers (*cf.* [1] as well as [9]), we were able to enrich **8′i** to an extent of up to 80% by irradiation of **8i** at 440 nm in C_6D_6. It reverted already at ambient temperature slowly to **8i**. In benzene, at 55°, **8′i** was transformed completely into **8i** within 3.7 h (see later).

[1]) We will report on such measurements later in this journal.

3. Structural and Spectroscopic Characterization of the New Donor-Acceptor-Substituted Heptalenes. – 3.1. *X-Ray Crystal Structures.* Crystal-structure analyses were performed of the 1-[(*E*)-2-pyrrolidinoethenyl]-substituted heptalene-4,5-dicarboxylates **8c** and **8i** (see *Fig. 2*), which crystallized in red tablets and red prisms, respectively, from AcOEt/pentane. Relevant structural parameters are listed in *Table 2*. The monoclinic crystals of **8c** were quite weakly diffracting. Therefore, there was a paucity of observed reflections (1953; *cf. Table 10*) in comparison with those of the triclinic crystals of **8i** (3452; *cf. Table 10*), which led to slightly less accurate structural parameters. Nevertheless, they are still in line with those of the starting heptalene-4,5-dicarboxylate **5a** (*cf. Table 2*). The parameters of **8i** are also compared with those of dimethyl 6,8,10-trimethyl-1-[(*E*)-2-phenylethenyl]methylheptalene-4,5-dicarboxylate

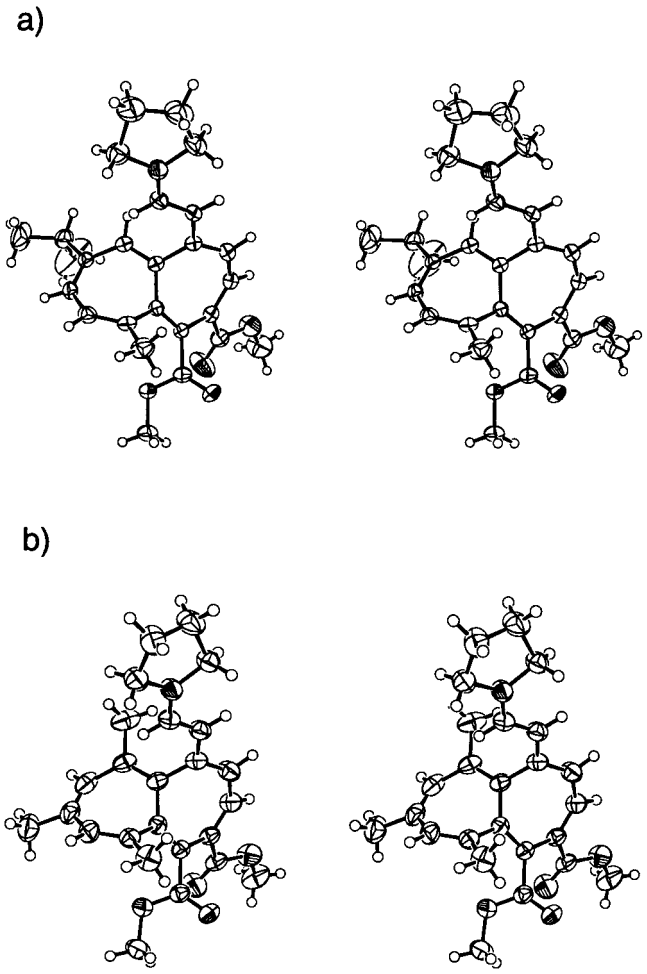

Fig. 2. *Stereoscopic view of the crystal structure of the two 1-[(*E*)-2-pyrrolidinoethenyl]-substituted heptalene-4,5-dicarboxylates* **8c** (*a*) *and* **8i** (*b*)

Table 2. *Relevant Structural Parameters of the X-Ray Crystal-Structure Analyses of the Heptalene-4,5-dicarboxylates* **8c** *and* **8i** *in Comparison to Those of* **5a** *and* **7b**[a])

Heptalene No. Parameter[c])	**8c**	**5a**[b])	**8i**	**7b**
Interatomic distances *d* [pm]				
C(1)–C(2)	136.0(5)	134.4(2)	136.5(3)	135.7(2)
C(1)–C(1′)	144.0(5)	–	143.4(3)	146.1(2)
C(1′)–C(2′)	135.1(5)	–	135.5(3)	133.0(3)
C(2′)–N	134.9(5)	–	134.6(3)	–
C(2)–C(3)	143.5(5)	144.3(2)	142.6(3)	144.0(2)
C(3)–C(4)	135.2(5)	135.0(2)	135.6(3)	136.1(2)
C(4)–C(5)	146.4(5)	147.6(2)	146.3(3)	146.6(2)
C(4)–C(1″)	149.1(5)	150.0(2)	149.1(3)	148.9(2)
C(5)–C(1‴)	150.2(5)	150.0(2)	150.6(3)	150.1(2)
C(1″)=O	118.8(5)	121.1(2)	119.7(2)	1212.5(2)
C(1‴)=O	119.5(2)	120.0(2)	120.0(2)	120.7(2)
C(5a)–C(10a)	148.3(2)	149.1(2)	148.0(2)	148.2(2)
Bond angles ϑ [°]				
C(2′)–N–C^N(2)	123.7(4)	–	124.4(2)	–
C^N(2)–N–C^N(5)	112.3(4)	–	112.4(2)	–
C(2′)–N–C^N(5)	123.6(4)	–	123.2(2)	–
Torsion angles Θ [°]				
C(2′)–C(1′)–C(1)–C(2)	177.3(5)	–	173.6(2)	179.3(2)
C(1)–C(2)–C(3)–C(4)	– 29.5(8)	– 32.9(2)	– 24.6(4)	– 29.3(3)
C(3)–C(4)–C(5)–C(5a)	32.5(7)	33.5(2)	30.7(3)	34.0(3)
C(1)–C(10a)–C(5a)–C(5)	– 65.3(5)	– 63.5(2)	– 65.8(2)	– 66.8(2)
C(6)–C(5a)–C(10a)–C(10)	– 64.8(5)	– 63.1(2)	– 68.0(2)	– 67.6(2)
C(5)–C(5a)–C(10a)–C(10)	116.7(5)	120.8(1)	112.9(2)	114.4(2)
C(1)–C(10a)–C(5a)–C(6)	113.3(4)	112.6(1)	113.3(2)	111.9(2)
C(3)–C(4)–C(1″)=O	– 172.9(5)	20.6(2)	– 160.9(2)	13.2(3)
C(1″)–C(4)–C(5)–C(1‴)	36.3(6)	32.1(2)	34.6(2)	37.2(2)
C(6)–C(7)–C(8)–C(9)	– 30.3(8)	– 34.2(2)	– 34.5(3)	– 36.6(3)
C(8)–C(9)–C(10)–C(10a)	31.3(7)	33.8(2)	32.8(4)	32.4(3)

[a]) Heptalene **7b** corresponds to **8i**, but with a Ph group at C(2′) instead of the pyrrolidino residue (*cf.* also **7a** in *Scheme 2*). Data are taken from [1a]. [b]) The structure was redetermined by X-ray crystal-structure analysis at 173(1) instead of 293 K in our former analysis [10]. Nevertheless, the deviations of both analyses are marginal. [c]) The torsion angles are given for the (*M*)-configuration of all heptalene cores.

(**7b**), in which the pyrrolidino group at C(2′) of **8i** is replaced by a Ph residue, which had been determined already earlier [1a].

The heptalene cores of all four structures exhibit alternating C–C and C=C bonds with the same lengths within the margins of the standard deviations. In other words, the pyrrolidino group at C(2′) with its strong π-donating N-atom, which is perfectly planar in **8c** as well as in **8i** according to the sum of its three valence angles (*cf. Table 2*), does not alter significantly the geometrical parameters of the heptalene skeleton. The Me substitution at C(10) of **8i** and **7b** causes a slightly larger twisted central s-*trans*-buta-1,3-dienyl unit (Θ(C(5)–C(5a)–C(10a)–C(10) = 112.9(2) and 114.4(2), resp.) in comparison to **8c** and **5a**, which carry a H-atom at C(10)

(Θ(C(5)–C(5a)–C(10a)–C(10) = 116.7(5) and 120.8(1), resp.). As a result, there is in **8c** a moderately larger extension of the heptalene core across the central σ-bond than in **8i**, *e.g.*, the s-*trans*-conformation of the ethenyl group with respect to C(1)=C(2) leads to an approach of H–C(2′) and the nearest H-atom of Me–C(6), resulting in a shorter interatomic distance of these H-atoms in **8c** (351 pm) than in **8i** (398 pm). This effect is also reflected in solution in the intensities of the ^{1}H-NOE effects between these H-atoms (see *Sect. 3.2*). A comparison of the torsion angles of the donor-acceptor-substituted s-*cis*-butadiene subunit C(1)=C(2)–C(3)=C(4) in **8c** and **8i** indicates the tendency of a decrease of this angle with the introduction of the strongly electron-donating (2-pyrrolidinoethenyl) moiety (*cf.* $\Theta = -32.9(2)^\circ$ of **5a** with $-29.5(8)^\circ$ of **8c** as well as $\Theta = -29.3(3)^\circ$ of **7b** with $-24.6(4)^\circ$ of **8i**). These effects are also recognizable in the ^{1}H-NMR spectra at the vicinal coupling constants of J(H–C(2), H–C(3)) of the heptalenes (see *Sect. 3.2*). In contrast to **5a** and **7b**, the donor-substituted heptalenes **8c** and **8i** display the most extended π-structure with respect to the electron-accepting E_{Me} group at C(4), which occupies s-*trans*-conformations in relation to the adjacent heptalene C(3)=C(4) bond, whereas corresponding s-*cis*-conformations are found in the crystal structures of **5a** and **7b** (*cf.* Θ(C(3)–C(4)–C(1″)=O = $-172.9(5)^\circ$ (**8c**) and $-160.9(2)^\circ$ (**8i**) with $20.6(2)^\circ$ (**5a**) and $13.2(3)^\circ$ (**7b**)). These s-*trans*-conformations play also the dominant role in solution as is demonstrated by NOE measurements of **8c** and **8i** (see *Sect. 3.2*).

3.2. *NMR Spectra.* The NMR data of all new donor-acceptor-substituted heptalene-5-carboxylates **8** are collected in *Tables 3–5*. The size of ^3J(H–C(1′),H–C(2′)) = 13.0–13.4 Hz in $CDCl_3$ or C_6D_6 indicates clearly that all heptalenes **8** possess the (*E*)-configuration at the dialkylamino-substituted ethenyl group at C(1). A closer inspection of the observable trend of the size of the vicinal coupling constants in the narrow range of 0.3 Hz reveals that ^3J is almost 13.1 Hz with the strongly electron-donating dialkylamino groups at C(2′), such as those in **8a**–**8c** and **8i**, whereas the weaker electron-donating groups, such as those in **8d** and **8e**, lead to ^3J values at the upper limit of 13.3–13.4 Hz. No solvent effects on ^3J are observable in the weakly polar solvents $CDCl_3$ and C_6D_6. However, in (D_6)DMSO, ^3J of **8c** falls slightly below 13.0 Hz. We interpret this effect as the result of a stronger accentuation of the dipolar character of the ground-state of **8c** due to the high polarity of (D_6)DMSO. Heptalene **8h** possesses a second, electron-accepting ethenyl side chain at C(4), which displays ^3J(H–C(1″),H–C(2″)) = 15.8 Hz, again, in full agreement with the (*E*)-configuration at this C=C bond.

^{1}H-NOE Measurements in C_6D_6 of **8c** and its higher substituted counterpart **8i**, with three and four substituents, respectively, at the *peri*-positions, are in conformity with the observation that both compounds prefer not only in the crystalline state but also in solution the s-*trans*-conformation at C(1)–C(1′), since strong reciprocal ^{1}H-NOE effects are observed between H–C(2) and H–C(1′) as well as between H–C(10) (**8c**) or Me–C(10) (**8i**) and H–C(2′). A moderate reciprocal ^{1}H-NOE effect is also recognizable between Me–C(6) and H–C(2′) of **8i**, which is again explained with a strong dominance of the discussed s-*trans*-conformation. This latter effect is in agreement with an interatomic H,H distance of 351 pm between the mentioned atoms in the crystal structure of **8i** (*cf. Sect. 3.1*). It is of interest to note that the discussed ^{1}H-NOE effect is much weaker for **8c** in C_6D_6 and almost not detectable for **8c** in

Table 3. *^{1}H-NMR Data of the Heptalene-4,5-dicarboxylates* **8** [a])[b])

	8a		**8b**		**8c**			**8d**		**8e**		**8i**		**8′i**[c])
H-Atom	$CDCl_3$	C_6D_6	$CDCl_3$	C_6D_6	$CDCl_3$	C_6D_6	(D_6)DMSO	$CDCl_3$	C_6D_6	$CDCl_3$	C_6D_6	$CDCl_3$	C_6D_6	C_6D_6
H−C(2)	5.890 (7.1(5))	5.936 (7.1(2))	5.878 (6.6)	5.916 (7.1(9))	5.867 (7.2(8))	5.983 (7.2(1))	5.876 (7.5(0))	5.896 (6.7)	5.956 (7.0(8))	5.959 (6.9(6))	5.974 (7.0(2))	6.030 (7.0(1))	6.133 (6.8(4))	6.846 (12.0)
H−C(3)	7.586 (7.1(6))	7.981 (7.0(8))	7.581 (7.1(2))	7.987 (7.0(2))	7.582 (7.2(3))	8.022 (7.1(1))	7.434 (7.4(3))	7.591 (7.1(2))	7.990 (7.0(4))	7.591 (6.9(3))	7.912 (6.9(4))	9.619 (6.9(7))	8.072 (6.8(1))	6.980 (12.0)
E_{Me}−C(4)	3.659	3.385	3.667	3.371	3.653	3.390	3.561	3.667	3.385	3.681	3.382	3.673	3.359	3.421
E_{Me}−C(5)	3.676	3.515	3.684	3.504	3.673	3.518	3.568	3.684	3.509	3.693	3.500	3.673	3.512	3.462
Me−C(6)	1.919	2.070	1.930	2.106	1.919	2.109	1.807	1.927	2.069	1.943	2.043	2.053 (1.1(7))	2.052	1.867
H−C(7)	6.183 (6.4(6), 1.3(2))	6.213 (6.4(4), 1.3(0))	6.180 (6.4(0), 1.2(1))	6.206 (6.4(8), 0.9(7))	6.177 (6.4(4))	6.237 (6.3(9))	6.197 (6.4(3))	6.207 (6.4(6), 1.2(2))	6.219 (6.4(4), 1.2(0))	6.196 (6.3(5))	6.214 (6.4(4), 1.3(0))	6.042	6.082	5.986
R^1−C(8)	6.273 (6.4(2))	6.270 (7.1)	6.278 (5.7)	6.254 (6.0)	6.268 (6.4(4))	6.286 (6.4(1))	6.260 (6.4(4))	6.274 (6.3(5))	6.277 (6.3(6))	6.293[d])	6.273 (6.4(5))	1.860 (1.3(1))	1.899	1.843
R^2−C(9)	2.448; 1.049; 1.020	2.277; 0.933; 0.916	2.448; 1.053; 1.026	2.268; 0.934; 0.913	2.442; 1.046; 1.021	2.293; 0.953; 0.930	2.460; 1.012; 0.967	2.454; 1.053; 1.026	2.275; 0.962; 0.949	2.467; 1.060; 1.036	2.283; 0.922; 0.914	6.139	6.150	6.068
R^1−C(10)	5.889	6.077	5.889	6.117	5.910	6.160	5.899	5.889	6.083	5.884	6.032	1.644	1.794	2.365
H−C(1′)	5.191 (13.1(0))	5.160 (13.1(5))	5.063 (13.0(9))	5.072 (13.1(2))	5.172 (13.0(6))	5.224 (13.0(8))	5.205 (12.9(5))	5.343 (13.3(3))	5.328 (13.3(8))	5.403 (13.4(6))	5.300 (13.4(6))	5.161 (13.0(8))	5.191 (13.1(0))	5.067 (13.8)
H−C(2′)	6.424 (13.0(8))	6.495 (13.1(3))	6.310 (13.0(4))	6.471 (13.0(2))	6.674 (13.0(6))	6.823 (13.0(8))	6.737 (12.9(5))	6.372 (13.3(3))	6.495 (13.3(8))	6.285 (13.2(3))	6.337 (13.4(6))	6.414 (13.0(7))	6.543 (13.1(1))	6.336 (13.8)
R^3−C(2′)	2.751	2.091	3.814(*t*) (H−C(2,4)); 2.284 (*quint.*) (H−C(3))	3.138 (*t*); 1.476 (*quint.*)	3.156 (*m*) (H−C(2,5)); 1.864 (*m*) (H−C(3,4))	2.585 (*m*); 1.177 (*m*)	3.152 (*m*) 1.816 (*m*)	3.009 (*m*) (H−C(2,6)); 1.544 (*m*) (H−C(3,4,5))	2.523 (*m*); 1.083 (*m*)	3.674 (*m*) (H−C(2,6)); 3.006 (*m*) (H−C(3,5))	3.204 (*t*); 2.412 (*t*)	3.155 (*m*) (H−C(2,5)); 1.876 (*m*) (H−C(3,4))	2.606 (*m*); 1.186 (*m*)	2.708 (*m*); 1.314 (*m*)

[a]) Spectra at 300 or 600 MHz; δ [ppm] with respect to the solvent signals at 7.260 ($CHCl_3$), 7.160 (C_6HD_5), and 2.500 ((D_5)DMSO). ^3J and ^4J [Hz] in parentheses; numbers in second parentheses represent the second, not secured decimal figures. [b]) For R^1, R^2, R^3 see *Table 1*. [c]) DBS Isomer of **8i**, *i.e.*, C(1) (**8i**) → C(5) (**8′i**), C(2) (**8i**) → C(4) (**8′i**) → C(3) (**8′i**), C(4) (**8i**) → C(2) (**8′i**), and so forth. [d]) Overlapping with the signal of H−C(1′).

Table 4. *^{13}C-NMR Data of the Heptalene-4,5-dicarboxylates* **8**[a])[b])

	8a		**8b**		**8c**		**8d**		**8e**		**8i**
C-Atom	$CDCl_3$	C_6D_6	$CDCl_3$	C_6D_6	$CDCl_3$	C_6D_6	$CDCl_3$	C_6D_6	$CDCl_3$	C_6D_6	C_6D_6
C(1)	145.83	145.49	144.98	144.83	146.18	145.98	145.92	145.57	144.59	144.71	144.94
C(2)	116.19	117.37	116.97	117.89	115.64	116.85	116.45	117.71	118.42	119.02	117.26
C(3)	144.44	143.96	142.21	141.92	140.96	140.98	144.14	143.83	143.22	143.30	140.26
C(4)	125.86	127.68	126.37	127.84	125.46	127.40	126.11	128.32	126.67	127.68	127.17
C(5)	124.36	126.00	124.35	126.00	124.50	126.19	124.30	125.99	124.12	125.69	125.15
C(5a)	140.63	140.81	140.95	140.95	140.25	140.36	140.86	141.08	141.74	141.59	142.82
C(6)	127.21	130.82	129.58	130.81	127.37	130.96	127.13	130.73	129.34	130.61	132.80
C(7)	127.31	127.72	127.37	127.84	127.30	127.84	127.32	127.69	127.35	128.19	129.41
C(8)	125.50	125.82	125.57	125.91	125.35	125.87	125.65	125.99	126.00	126.20	139.48
C(9)	147.90	148.20	147.94	148.14	147.83	148.15	147.98	148.26	148.04	148.29	130.69
C(10)	125.21	125.82	125.26	125.91	125.18	125.77	125.19	125.79	125.29	125.86	130.39
C(10a)	129.49	128.67	127.19	128.54	129.57	128.84	129.40	128.55	127.59	129.11	123.33
C(1′)	99.45	100.47	100.91	101.63	99.86	100.89	99.80	100.94	101.81	102.33	99.17
C(2′)	140.91	140.81	140.82	140.76	140.25	139.89	140.86	140.73	140.53	140.49	139.84
$R^3_2N-C(2')$	40.61	39.94	52.10 (C(2,4)); 16.69 (C(3))	51.77 16.60	49.06 (C(2,5)); 25.06 (C(3,4))	49.18 25.35	49.80 (C(2,6)); 25.24 (C(3,5)); 24.15 (C(4))	49.96 25.71; 24.60	66.08 (C(2,6)); 48.68 (C(3,5))	66.00 48.64	48.85 (C(2,5)); 24.96 (C(3,4))
$E_{Me}-C(4)$	167.94	167.80	167.90	167.75	167.96	167.87	167.96	168.77	167.78	167.66	168.00
	51.58	51.22	51.64	51.23	51.51	51.21	51.56	51.23	51.73	51.34	51.13
$E_{Me}-C(5)$	168.50	168.17	168.45	168.14	168.58	168.31	168.50	168.10	168.25	167.96	168.20
	51.85	51.46	51.88	51.46	51.81	51.48	51.85	51.45	51.91	51.52	51.41
Me–C(6)	21.64	22.01	21.66	22.02	21.65	22.13	21.59	21.99	21.64	21.96	21.67
Me–C(8)	–	–	–	–	–	–	–	–	–	–	25.12
i-Pr–C(9)	35.43	35.76	35.46	35.76	35.41	35.79	35.46	35.76	35.43	35.73	–
	23.10;	23.13;	23.12;	23.12;	23.09;	23.17;	23.13;	23.13;	23.13;	23.13;	–
	22.29	22.45	22.31	22.44	22.27	22.40	22.31	22.45	22.28	22.45	
Me–C(10)	–	–	–	–	–	–	–	–	–	–	19.27

[a]) ^{13}C-NMR spectra at 75 or 150 MHz; δ [ppm] with respect to *C*DCl_3 at 77.00 and C_6D_6 at 128.00, respectively. [b]) For R^3, see *Table 1*.

Table 5. *Relevant NMR Data of the 1-[(*E*)-2-Pyrrolidinoethenyl]heptalene-5-carboxylates* **8**[a])

	8f		**8g**		**8h**	
	^{1}H[b])	^{13}C	^{1}H	^{13}C	^{1}H	^{13}C
H–C(2)	5.968 (7.0(7))	116.80	5.675 (7.2(6))	116.14	5.907 (7.0(8))	115.05
H–C(3)	6.90[c])	148.86	7.003 (7.2(2))	144.52	6.708 (7.1(9))	140.33
E_{Me}–C(5)	3.608	168.25; 51.73	3.490	166.15; 51.89	3.416	168.76; 51.59
Me–C(6)	2.105	22.16	2.040	21.97	2.068	21.97
H–C(7)	6.221(6.6(0))	128.32	6.195 (6.4(6))	128.29	6.215 (6.4)(1))	127.56
H–C(8)	6.269 (6.1(5))	126.48	6.260 (6.4(3))	126.13	6.300 (6.3(5))	125.69
i-Pr–C(9)	2.268; 0.922; 0.898	35.83; 23.09; 22.35	2.273; 0.940; 0.911	35.84; 23.17; 22.31	2.299; 0.960; 0.937	35.87; 23.19; 22.43
H–C(10)	6.136	126.09	6.087	125.88	6.165	125.60
H–C(1′)	5.238 (13.0(0))	101.10	5.133 (13.0(8))	100.32	5.219 (13.1(4))	101.16
H–C(2′)	6.89[c])	140.98	6.780 (13.0(8))	140.61	6.777 (13.1(4))	139.29
C_4H_8N–C(2′)						
H_2C(2,5)	2.539(*m*)	48.71	2.522	48.79	2.590	48.76
H_2C(3,4)	1.120(*m*)	24.86	1.128	24.87	1.192	24.96
H–C(1″)	9.387	190.99	–	121.12	7.813 (15.8(1))	148.48
H–C(2″)	–	–	–	–	6.149 (15.8(3))	118.15
E_{Me}–C(2″)	–	–	–	–	3.410	167.58; 50.78

[a]) Spectra in $CDCl_3$ at 300 and 75 MHz, respectively; δ [ppm] with respect to 7.160 ($CHCl_3$) or 77.00 ppm ($CDCl_3$). [b]) In parentheses ^3J [Hz]; numbers in second parentheses represent the second, not secured decimal figures. [c]) Overlapping of the signals of H–C(3) and H–C(2′).

(D_6)DMSO. These findings are in agreement with the more extended heptalene core of **8c**, which leads to an interatomic H,H distance between H–C(2′) and Me–C(6) of 398 pm in the crystalline state of **8c** (*cf. Sect. 3.1*). Moreover, it seems that the heptalene core of **8c** in (D_6)DMSO is still a little more extended due to a stronger dipolar interaction of the pyrrolidino group at C(2′) and E_{Me}–C(4), which will flatten the heptalene skeleton at the donor-acceptor-substituted ring. This extension is also indicated by an increase of the ^3J(H–C(2),H–C(3)) value of **8c** in C_6D_6 (or $CDCl_3$) and in (D_6)DMSO from 7.2 to 7.4 Hz, in contrast to ^3J(H–C(7),H–C(8)) = 6.4 Hz in all three solvents.

3.3. *IR Spectra*. We studied the effect of enamine formation at C(1) on the C=O stretching frequencies in the case of the heptalene-4,5-dicarboxylates **5a** and **5b** and their corresponding 1-[(*E*)-2-pyrrolidinoethenyl] derivatives **8c** and **8i**, respectively. The extended region of the C=O stretching vibrations in the IR spectra of **5a**/**8c** and **5b**/**8i**, measured at the same concentration, is displayed in *Figs. 3*,*a* and *b*. The relevant wavenumbers are listed in *Table 6*. The starting diesters **5a** and **5b** exhibit an almost symmetrical absorption band at 1720 and 1714 cm^{-1}, respectively, for both ester groups. The band position is shifted to 1708 and 1707 cm^{-1} for the enamine diesters **8c** and **8i**, respectively, in agreement with the fact that the strong electron-donating enamine moiety at C(1) is conjugatively coupled with E_{Me}–C(4) *via* the heptalene π-core. A closer inspection of the band shape of the stretching vibration of the ester groups in **8c** and **8i** uncovers a slight asymmetry of the bands, which is more pronounced for **8i** than **8c**. One recognizes for **8i** a shoulder at *ca*. 1722 cm^{-1} with the position of the main band

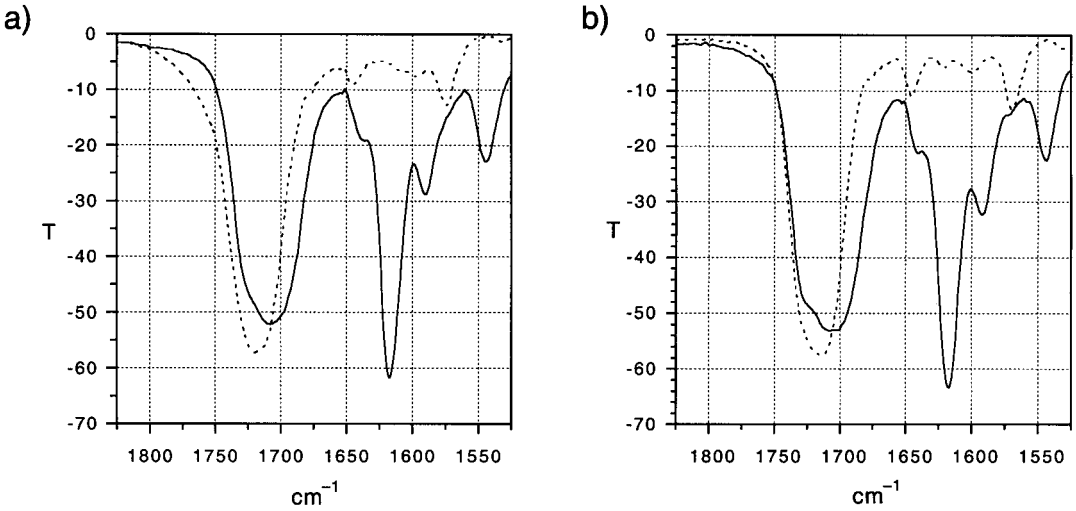

Fig. 3. *C=O Stretching region in the IR spectra of the 1-[(*E*)-2-pyrrolidinoethenyl]-substituted heptalene-4,5-dicarboxylates* **8c** (*a:* solid line) *and* **8i** (*b:* solid line) *and their corresponding heptalene progenitors* **5a** (*a:* dotted line) *and* **5b** (*b:* dotted line), *respectively, in* $CHCl_3$ ($c = 5 \cdot 10^{-5}$ mol/l)

Table 6. *Relevant Wavenumbers in the IR Spectra of* **8c** *and* ***8i***, *and Their Progenitor Diesters* **5a** *and* **5b**, *Respectively*[a])

Compound	$\tilde{\nu}$ [cm^{-1}]	
	$-C$(OMe)=O	$R_2^3N-CH=CH$[b])
5a	1720	–
8c	*ca.* 1720 (sh), 1708	1617.5
5b	1714	–
8i	*ca.* 1722 (sh), 1707	1617.5

[a]) In $CHCl_3$, $c = 5 \cdot 10^{-5}$ mol·l^{-1}; see also *Fig. 6.* [b]) (*E*)-Configuration; see *Table 1.*

at 1707 cm^{-1}. This effect is much less visible in the IR spectrum of the enamine diester **8c**. We consider these observed tendencies as the result of the discussed donor-acceptor interaction in the ground-state of **8c** and **8i**, which shifts only the band position of the conjugatively involved ester groups at C(4) to lower frequencies, whereas those of the ester groups at C(5) remain unaffected. The narrow band of the C=C stretching vibration of the (*E*)-configured ethenyl group of **8c** and **8i** appears for both esters at the same wavenumber (1617.5), thereby indicating that the donor-acceptor π-interaction must be of the same order in the ground-state of both enamine-substituted diesters. The wavenumber of the C=C stretching vibration of the 2-pyrrolidinoethenyl group of **8c** and **8i** is in good agreement with those of other enamines with comparable structural elements (*cf.* [11]).

3.4. *UV/VIS Spectra*. The spectra of **8c** and **8i** as typical examples of the new 1-[(*E*)-2-(dialkylamino)ethenyl]-substituted heptalene-5-carboxylates with an electron-acceptor group at C(4) are displayed in *Figs. 4* and *5*, and the data of the two longest-wavelength absorption bands of all heptalenes **8** are listed in *Table 7.* A correlation of

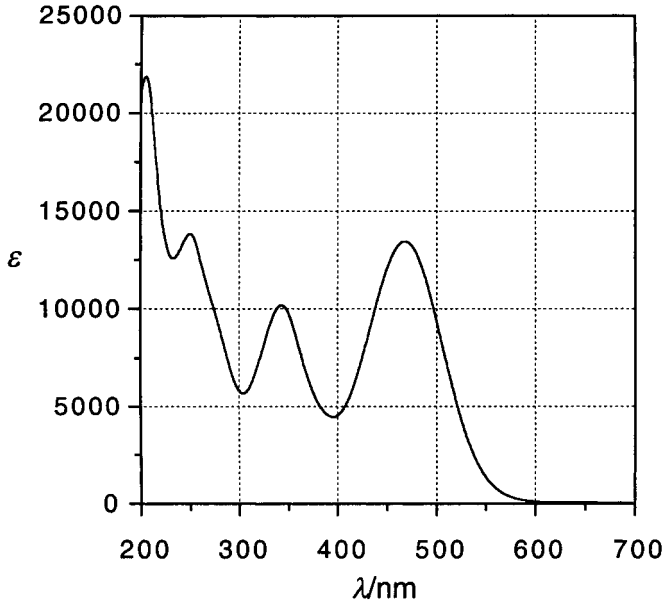

Fig. 4. *UV/VIS Spectrum of dimethyl 6,8,10-trimethyl-1-[(*E*)-2-pyrrolidinoethenyl]heptalene-4,5-dicarboxylate* (**8i**) *in MeCN*

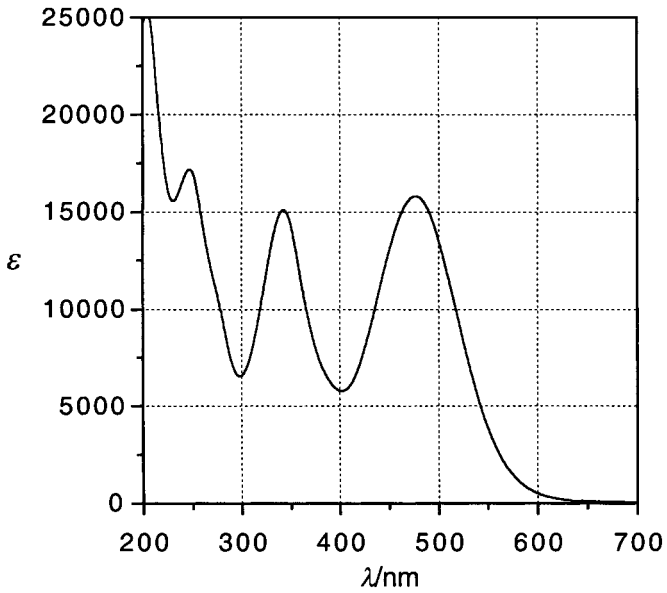

Fig. 5. *UV/VIS Spectrum of dimethyl 9-isopropyl-6-methyl-1-[(*E*)-2-pyrrolidinoethenyl]heptalene-4,5-dicarboxylate* (**8c**) *in MeCN*

Table 7. *Longest-Wavelength Heptalene-Absorption Bands of the 1-[(*E*)-2-(Dialkylamino)ethenyl]heptalene-5-carboxylates* **8**[a])

R^1	R^2	R^3	A	No.	λ_{max} [nm] (ε)	λ_{max} [nm] (ε)
H	i-Pr	Me	E_{Me}	**8a**	338.2 (12900)	466.5 (11000)
H	i-Pr	$-(CH_2)_3-$	E_{Me}	**8b**	339.7 (17000)	468.8 (15600)
H	i-Pr	$-(CH_2)_4-$	E_{Me}	**8c**	342.6 (15100)	476.5 (15800)
H	i-Pr	$-(CH_2)_5-$	E_{Me}	**8d**	343.0 (10200)	467.6 (14400)
H	i-Pr	$-(CH_2)_4O-$	E_{Me}	**8e**	339.8 (15600)	459.0 (16400)
H	i-Pr	$-(CH_2)_4-$	CHO	**8f**	355.2 (13800)	501.0 (19400)
H	i-Pr	$-(CH_2)_4-$	CN	**8g**	350.0 (16300)	490.9 (15400)
H	i-Pr	$-(CH_2)_4-$	$CH=CHE_{Me}$	**8h**	360.2 (8500)	494.3 (12900)
Me	H	$-(CH_2)_4-$	E_{Me}	**8i**	343.6 (10100)	468.2 (13400)
Me	H	Me	E_{Me}	**8k**	340.6 (13600)	459.0 (16300)

[a]) In MeCN; for the positions of the substituents, see *Table 1*.

the absorption bands of **8i** with those of 1,3,5,6,8,10-hexamethylheptalene (**14**), and the heptalene-4,5-dicarboxylates **5b** and **7b** (*cf. Scheme 2*, *Table 8*, and *Figs. 6* and *7*), as well as their DBS isomers **5′b** and **7′b**, which are also included in *Table 8*, reveals that the heptalene band I is liable to the strongest batho-, hyper-, and solvatochromic effects in the series of the four heptalenes. It seems that the heptalene band II of **8i**, which is clearly seen in the case of **14** at 310 nm and still recognizable as a shoulder in the case of **5b** and the 1-[(*E*)-styryl]-substituted heptalene **7b** at 320 and 355 nm, respectively, is buried under the strong heptalene band III. It appears in hexane at 330 nm and in MeCN at 343 nm. Irradiation of **8i** in hexane (λ_{max} (I) 430.8 nm) or in MeCN (λ_{max} (I)

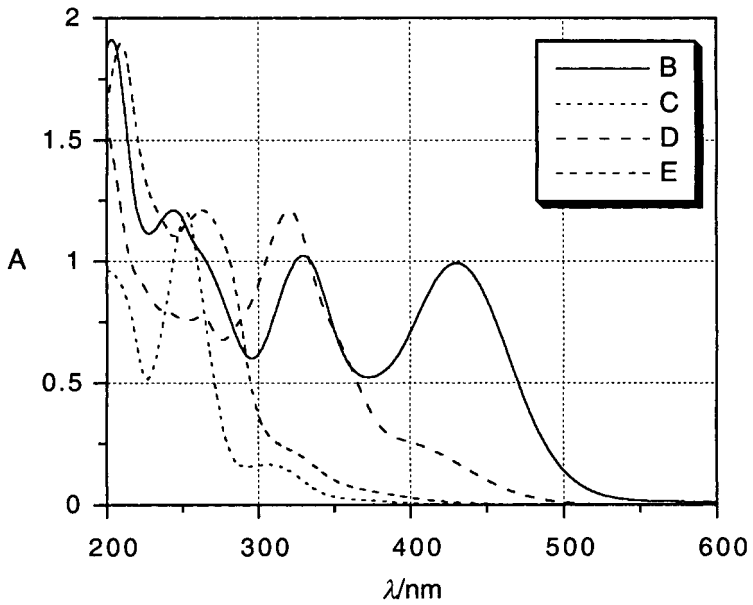

Fig. 6. *Comparison of the UV/VIS spectra of 1,3,5,6,8,10-hexamethylheptalene* (**14**; curve *E*), **5b** (curve *D*), **7b** (curve *C*), *and* **8i** (curve *B*) *in hexane* (*cf. Table 8*)

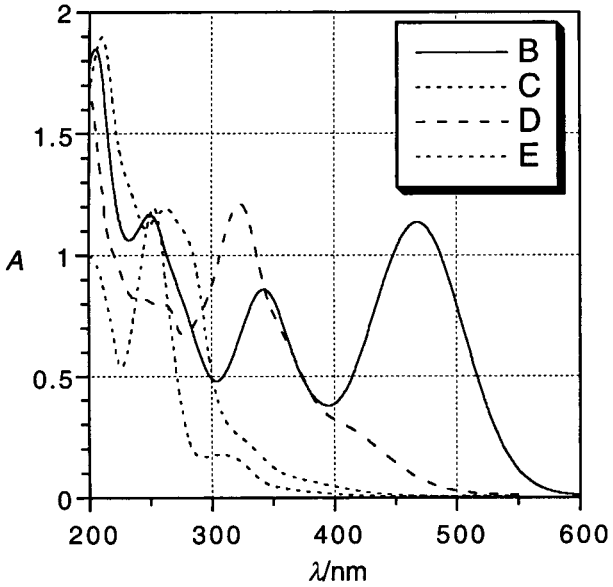

Fig. 7. *Comparison of the UV/VIS spectra of 1,3,5,6,8,10-hexamethylheptalene* (**14**), **5b**, **7b**, *and* **8i** *in MeCN* (B–E as in *Fig. 6*; *cf. Table 8*)

468.2 nm) with the light of a tungsten lamp (λ_{emiss} 467 and 650 nm) leads in both solvents to the rapid establishment of a photostationary state of **8i** and **8′i**, which is composed of *ca.* 85% of **8′i** and 15% of **8i** (*cf. Fig. 8*). On standing at room temperature or more rapidly on heating at 50°, **8′i** in the photostationary state mixture reverts quantitatively to **8i** with the energetically favorable conjugative interaction of the donor-acceptor substituents at C(1) and C(4). Heptalenes **8i** and **8′i** can be separated by HPLC with hexane/CH_2Cl_2 65 : 35 without thermal isomerization of **8′i**. The UV/VIS spectra of both heptalenes in the eluant mixture are displayed in *Figs. 9* and *10*. In contrast to **8i**, which exhibits heptalene band I as the dominant electronic absorption at 451 nm, heptalene band I appears in the spectrum of **8′i** as the weakest electronic absorption at 445 nm, in full agreement with our earlier results with other heptalenes (*cf.* [1]). The spectra of **8i** and **8′i** in hexane/CH_2Cl_2 exhibit a slightly asymmetric heptalene band III at *ca.* 350–360 nm, which might be caused by heptalene band II, since it has to expected in this region according to the correlation with the other heptalenes (*cf. Figs. 6* and *7* as well as *Table 8*; see [1] for further examples).

An inspection of *Figs. 4* and *5* and *Table 7* shows that heptalene band I of **8c** and **8i** in MeCN appears at 476.5 and 468.2 nm, respectively, *i.e.*, in going from heptalene **8c** with three *peri*-substituents to heptalene **8i** with four, heptalene band I is hypsochromically shifted by 8.3 nm[2]). A similar effect is observed for the heptalene pair **8a** and **8k** in MeCN, where the hypsochromic shift of heptalene band I is a little smaller and amounts to 7.5 nm (*cf. Table 7*). We interpret these hypsochromic shifts of heptalene band I as in

---

[2]) In hexane, the shift difference between **8c** (λ_{max}(I) = 437.8 nm) and **8i** (λ_{max} (I) = 430.8 nm; *cf. Table 9*) amounts to 7.0 nm.

Table 8. *Absorption Bands in the UV/VIS Spectra of Substituted Heptalenes in Comparison with Those of 1,3,5,6,8,10-Hexamethylheptalene* (**14**)[a])

Compound	Solvent	Band λ [nm]			
		I	II	III	IV[c])
14	hexane	*ca.* 360 (sh)	310	252[d])	*ca.* 200
	MeCN	*ca.* 360 (sh)	309	253	202
5b	hexane	*ca.* 370 (sh)	*ca.* 320 (sh)	*ca.* 280 (sh)/261	*ca.* 236 (sh)/212
	MeCN	*ca.* 370 (sh)	*ca.* 325 (sh)	*ca.* 281 (sh)/263	*ca.* 236 (sh)/210
5′b	hexane	390	*ca.* 318 (sh)	268	*ca.* 233/214
7b	hexane	*ca.* 400 (sh)	*ca.* 355 (sh)	321	263/*ca.* 220 (sh)
	MeCN	*ca.* 400 (sh)	*ca.* 355 (sh)	322	263/230/*ca.* 220 (sh)
7′b	hexane	*ca.* 400	345 (sh)	285	235/*ca.* 215 (sh)
8i	hexane	431	–[e])	330	*ca.* 263 (sh)/245/204
	hexaneCH_2Cl_2[f])	451	*ca.* 360 ?[g])	339	267
	MeCN	468	–[e])	343	*ca.* 265 (sh)/250/205
8′i	hexane	427	–[e])	331	*ca.* 290 (sh)/*ca.* 275 (sh)/245
	hexane/CH_2Cl_2[f])	445	*ca.* 350 ?[g])	334	272
	MeCN	465	–[e])	338	259

[a]) See also *Figs. 4–6*. The UV/VIS data of **14**, **5b**, **7b**, and their DBS isomers **5′a** and **7′b** in hexane have been taken from [1]. [b]) For band assignments, which have been secured by CD measurements in hexane for **14**, **5b**, **7b**, and the DBS isomers, see [1]. [c]) Under band IV, all electronic transition beyond band III are listed. [d]) The CD spectrum of **14** exhibits the main *Cotton* effect at 249 nm with sh at 269 and 238 nm, respectively [1]. [e]) Heptalene band II not recognizable, since the shape of band I and III is almost symmetric (*cf. Figs. 4* and *5*). [f]) HPLC Eluant mixture of 65% of hexane and 35% CH_2Cl_2. [g]) Tentative assignment according to the slightly asymmetric shape of heptalene band III of **8i** and **8′i** (*cf. Fig. 6*, *a* and *b*).

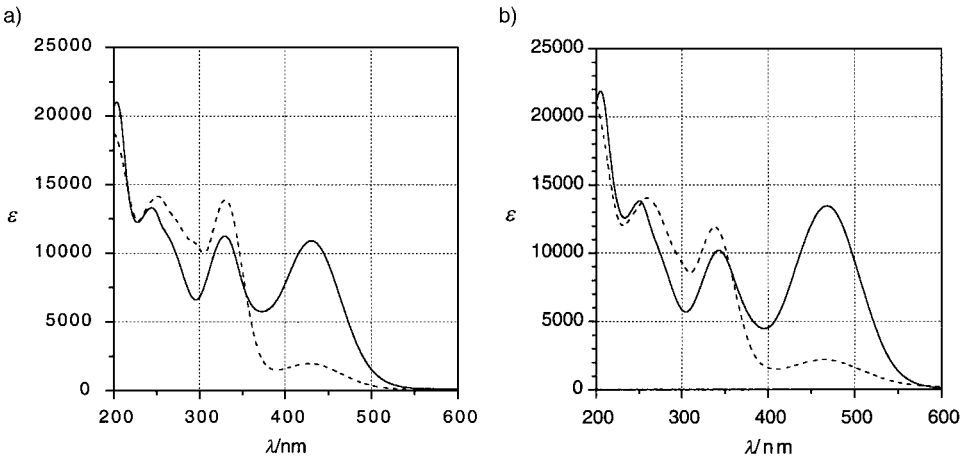

Fig. 8. *UV/VIS Spectrum of* **8i** *in hexane* (*a*) *and in MeCN* (*b*) *before* (solid line) *and after irradiation* (dotted line) *with light of a tungsten lamp*

the case of benzo- and furano-anellated heptalenes (*cf.* [7][12] and [13], resp.), and other heptalenes (*cf.* [1][14]) as a subtle measure of the degree of twisting of the heptalene skeleton, especially at the directly involved s-*cis*-butadiene subunit

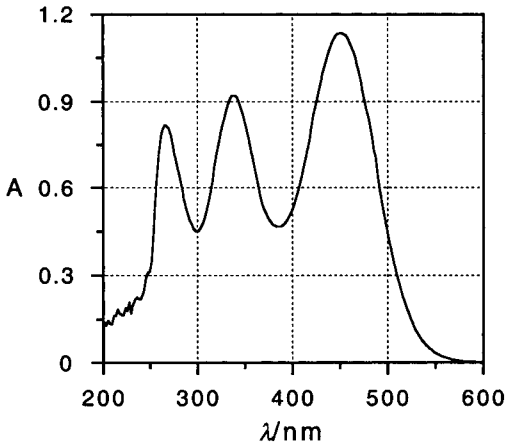

Fig. 9. *UV/VIS Spectrum of* **8i** *in hexane/CH_2Cl_2 65:35 measured with a photodiode detector after HPLC separation from* **8′i**

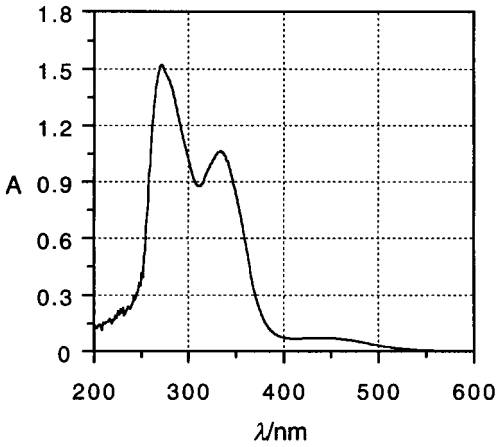

Fig. 10. *UV/VIS Spectrum of* **8′i** *in hexane/CH_2Cl_2 65:35 measured with a photodiode detector after HPLC separation from* **8i**

C(1)=C(2)−C(3)=C(4). Indeed, in solution ($CDCl_3$ or C_6D_6), ^3J(H−C(2),H−C(3)) of **8c** (in average 7.2 Hz) is distinctly larger than for **8i** (in average 6.9 Hz; *cf. Table 3*), indicating a smaller torsion angle of the regarded subunit for **8i** in contrast to **8c**. Interestingly, ^3J(H−C(2),H−C(3)) of **8c** is further increased to 7.5 Hz in (D_6)DMSO. It seems, therefore, that the polar ground-state of **8c** is additionally accentuated by enhanced solvation in strongly polar solvents such as DMSO, thus leading to a higher degree of conjugative interaction of the donor and acceptor substituents, which will diminish Θ(C(1)=C(2)−C(3)=C(4)) and, in turn, Θ(H−C(2)−C(3)−H).

The π-donor and π-acceptor substituents at C(1) and C(4) of **8** exhibit the expected pronounced influence on the position and intensity of the heptalene band I (*cf. Table 7*). On the other hand, the position of heptalene band III is much less affected by

the substituents. The position of heptalene band I of the heptalene-4,5-dicarboxylates **8a**–**8e** with the same acceptor group at C(4) (MeOCO), but different *N*,*N*-dialkylamino groups in the side chain at C(1), reflects the π-donor quality of the amino groups. The observed ranking pyrrolidino > azetidino > piperidino > dimethylamino > morpholino is in full agreement with the UV data of acyclic and cyclic enamines and dienamines (*cf.* [11] and specifically [15]) or the oxidation potentials of corresponding enamines [16]. One may ask to what extent the heptalene π-system with its comparably small energy gap between its HOMO and LUMO (*cf.* [1]) acts upon the position of the longest-wavelength absorption band of the acceptor-substituted enamines. Three examples are displayed in *Scheme 4*. They demonstrate impressively that, in comparison with the open-chain enamine **15** [17] with the same number of C=C bonds between donor and acceptor group, the heptalene π-skeleton, represented by **8l**, adds an increment of >70 nm to the longest-wavelength absorption band. Indeed, **8f**, our reference compound, shows heptalene band I in MeCN at 501 nm (*Table 7*). However, for a fair comparison, we have to take into account the better donor quality of the pyrrolidino group in relation to a Me_2N group at C(2′), which amounts to an increment of $+10$ nm in our heptalenes (*cf.* **8a** and **8c** in *Table 7*)[3]. A comparison of **8l** and derivative **16** [18] with the closest related aromatic 10e π-system reveals again the superiority of the heptalene 12e π-system with an incremental contribution of still >50 nm.

Scheme 4

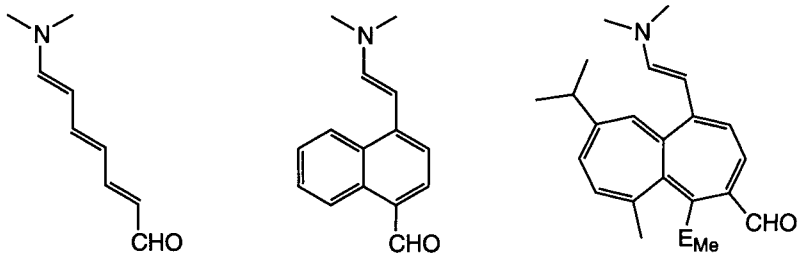

15 **16** **8l**

λ_{max} (MeCN)[a]) 418 nm [17] 438 nm [18] 491 nm[b])

[a]) Longest-wavelength absorption bands. [b]) Band position derived from **8f** (see text).

For a closer characterization of the ground-state and lowest-lying excited state that causes the strong hyperchromic effect on the donor-acceptor-substituted heptalenes **8**, we studied the solvatochromism of heptalene band I of **8i** in a number of solvents (*cf. Table 9* as well as *Figs. 6* and *7*). The observed maximum solvatochromic shift spans >43 nm in the range of 431 (hexane) – 474.5 nm (DMSO), and is comparable to those of donor-acceptor-substituted aromatic compounds (*cf. Table 9*) such as DEANB

[3]) The additional E_{Me} group at C(5) has no significant influence on the position of heptalene band I as we know from other investigations with comparable heptalenes carrying a Me group at C(5) [18].

(52 nm; range 359–411.5 nm) or DMANS (64 nm; range 391.5–455.5 nm) with typical charge-transfer (CT) excited states. Indeed, heptalene band I of **8i** shows an excellent linear correlation with the CT band of DEANB or DMANS (*cf. Figs. 11* and *12*), whereby the correlation with DMANS with a similar spatial extension of the relevant structural elements as **8i** is slightly better (*cf. Table 9*). That it is indeed the CT character of the excited state and not the polarity of the ground state, which governs the longest-wavelength absorption of heptalenes **8**, is demonstrated by the poorer linear correlation coefficients of heptalene band I with the $E_T(30)$ values of *Dimroth-Reichardt*'s pyridinium-phenolate as well as the E_T values of phenol blue (*cf. Table 9*), which both characterize ground-state polarities due to their zwitterionic structure or high degree of zwitterionic contribution to their ground-state structure as in the case of phenol blue (*cf.* [22]). We conclude, therefore, from our observations that the heptalenes **8** possess a ground-state polarity that is strongly enhanced in their lowest excited state due to the CT character of the considered electronic transition. The orbital symmetry of the HOMO and LUMO of planar D_{2h}-heptalene with delocalized π-bonds (*cf.* Fig. 12 in [1a]) is indeed in conformity with a CT excitation across the heptalene skeleton, which should not be altered fundamentally for twisted C_2-heptalene with localized π-bonds (*cf.* [23]). Moreover, due to the localization of the π-bonds in heptalenes, π-substituents, in 1,2 or 1,4 relation at one of the seven-membered rings, may interact in-phase or out-of-phase with the excited state, which should lead to strong or weak oscillator strengths of the considered electronic transition as has been demonstrated already in our earlier publications [1] as well as here, specifically in the case of **8i** and **8′i**.

Table 9. *Solvent Dependence of the Position of Heptalene Band I of Heptalene-4,5-dicarboxylate* **8i** *in Comparison with Those of the Longest-Wavelength Absorptions of DEANB, DMANS, and Phenol Blue*[a])

Solvent	λ [nm]			Phenol Blue[d])
	8i	DEANB[b]) λ [nm]	DMANS[c]) λ [nm]	E_T [kcal/mol]
Hexane	430.8	*359.3*	391.5	51.96
Benzene	448.3	*389.3*	424.0	49.73
Toluene	447.5	*387.2*	422.0	–
CCl_4	441.3	374.5	407.5	50.61
CH_2Cl_2	466.9	*399.3*	441.5	48.46
THF	453.9	390.5	429.0	48.72
Dioxane	449.8	388.0	423.5	–
Pyridine	467.5	403.5	448.0	47.98
Acetone	460.0	*396.2*	433.5	49.14
MeCN	468.2	400.5	439.0	48.97
AcOEt	450.3	388.5	422.0	49.98
DMF	469.4	405.5	446.0	48.06
DMSO	474.5	411.5	455.5	47.26
Corr. Coeff. r^2	–	0.939	0.962	0.905 (0.892)[f])

[a]) DEANB = 4-(Diethylamino)nitrobenzene; DMANS = (*E*)-4-(dimethylamino)-β-nitrostyrene; phenol blue = *N*-[4-(dimethylamino)phenyl]-*p*-benzoquinonimine. [b]) Values taken from [19]; own measurements in italics. [c]) Values taken from [20]. [d]) Transition energies (E_T) taken from [21]. [f]) In parentheses correlation coefficient (r^2) from the linear regression analysis of **8** and *Dimroth-Reichardt*'s $E_T(30)$ values (*cf.* [22]).

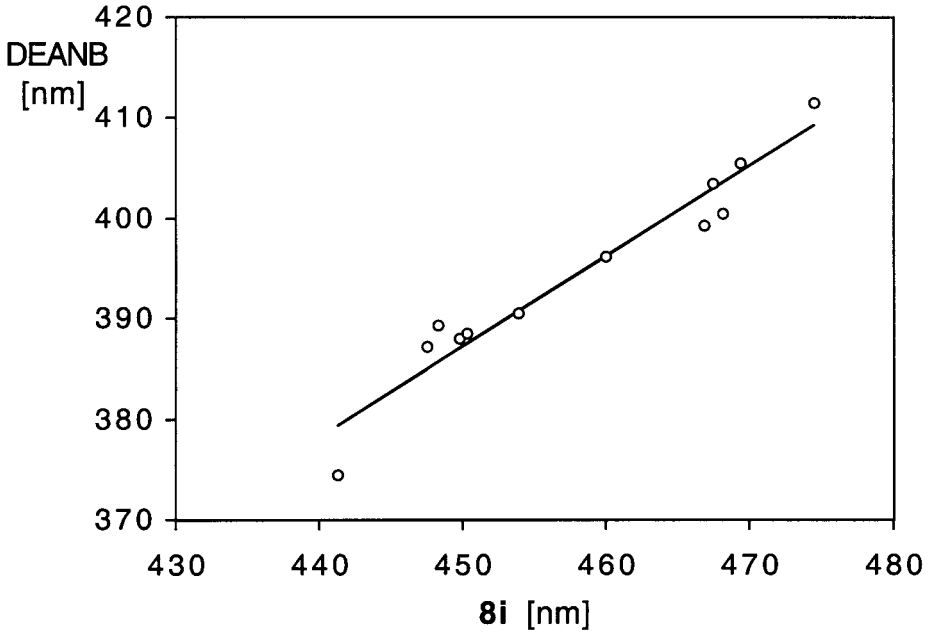

Fig. 11. *Solvent dependence of heptalene band I of* **8i** *and the CT band of 1-(diethylamino)-4-nitrobenzene* (DEANB; *cf. Table 9*)

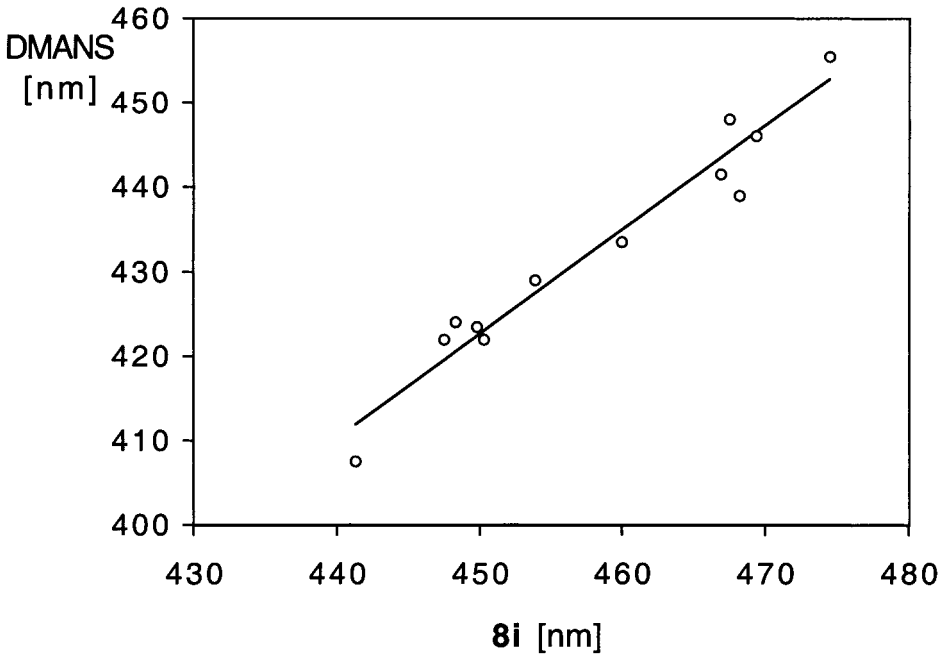

Fig. 12. *Solvent dependence of heptalene band I of* **8i** *and the CT band of* (E)*-4-(dimethylamino)-β-nitrostyrene* (DMANS; *cf. Table 9*)

We thank our NMR laboratory, in particular *Nadja Walch* and Dr. *Gudrun Hopp*, for specific NMR measurements, Dr. *Anthony Linden* for the X-ray crystal-structure analyses, and Dipl.-Chem. *Thomas Landmesser* for providing heptalene-4,5-dicarboxylate **5b**. Financial support of this work by the *Swiss National Science Foundation* is gratefully acknowledged. *Ph. O.* thanks especially the *Dr. Helmut Legerlotz-Stiftung* for a postdoctoral scholarship.

Experimental Part

General. See [1]. 1-(Diethylamino)-4-nitrobenzene (DEANB) was synthesized according to [19]. TLC: Al foils pre-coated with silica gel *60 F_{254}* (*Merck*). Column chromatography (CC): silica gel *60* (40–63 μm; *Chemie Uetikon AG*). UV/VIS Spectra: *Perkin-Elmer* spectrophotometer (model *Lambda 9*), λ in nm ($\log \varepsilon$). IR Spectra: on a *Perkin-Elmer* spectrophotometer (model *FT-IR 1600*), $\tilde{\nu}_{max}$ in cm^{-1}. ^1H- and ^{13}C-NMR Spectra: *Bruker* instruments (*AC 300*, *ARX 300*, *AMX 600*) in $CDCl_3$ or C_6D_6; δ (ppm); J in Hz; ^1H reference: $CHCl_3$ at 7.260 and C_6HD_5 at 7.160; ^{13}C reference: $CDCl_3$ at 77.00 and C_6D_6 at 128.00.

1. Synthesis of Donor-Acceptor-Substituted Heptalenes. – 1.1. *Methyl 4-Cyano-9-isopropyl-1,6-dimethylheptalene-5-carboxylate* (**11**). A soln. of formyl-ester **10** (0.30 g, 1.00 mmol) [1][7] in pyridine (0.5 ml) was added to $NH_2OH \cdot HCl$ (0.084 g, 1.20 mmol) in H_2O (0.25 ml), and the mixture was stirred at r.t. After 1 h, $CuSO_4 \cdot 5\,H_2O$ (0.050 g, 0.20 mmol) and Me_3N (0.21 g, 2.10 mmol) in CH_2Cl_2 (2 ml) were added. To this mixture, dicyclohexylcarbodiimide (DCC; 0.247 g, 1.20 mmol) was added. After stirring during 2 h, the excess of DCC was destroyed with HCOOH (0.17 ml). The mixture was diluted with Et_2O and washed 3 times with H_2O. The org. phase was dried ($MgSO_4$). The solvent was removed, and the residue was purified by CC (silica gel; hexane/Et_2O 1:1) to give pure **11** (0.025 g, 8%). Yellow crystals. M.p. 81.7°. R_f (hexane/Et_2O 1:1) 0.53. IR (KBr): 2958*s*, 2868*w*, 2214*m* (C≡N), 1717*s* (MeOC=O), 1638*w*, 1560*w*, 1429*m*, 1287*s*, 1238*w*, 1192*m*, 1055*s*, 845*m*, 638*m*. ^1H-NMR (300 MHz, $CDCl_3$): 7.03 (*dq*-like, $^3J = 6.2$, $^5J = 1.0$, H–C(3)); 6.30 (*d*, $^3J = 6.6$, H–C(8)); 6.17 (*dq*-like, $^3J = 6.6$, $^4J = 1.3$, H–C(7)); 6.11 (*dq*-like, $^3J = 6.2$, $^4J = 1.3$, H–C(2)); 5.87 (*s*, H–C(6)); 3.81 (*s*, MeOCO); 2.51 (*sept.*, $J = 6.9$, Me_2CH); 2.08 (*t*-like, $\Sigma^4J + {}^3J = 2.4$, Me–C(1)); 2.02 (*s*, Me–C(6)); 1.11/1.08 (2*d*, $J = 6.9$, 6.8, Me_2CH). ^{13}C-NMR (75 MHz, $CDCl_3$): 165.43 (*s*, MeO*C*O); 148.90 (*s*); 146.97 (*s*); 145.63 (*s*); 144.63 (*d*); 130.41 (*s*); 128.42 (*s*); 128.05 (*d*); 126.61 (*d*); 125.59 (*d*); 125.02 (*d*); 121.45 (*s*); 118.91 (*s*); 114.46 (*s*, C≡N); 52.37 (*s*, *Me*OCO); 35.62 (*d*, Me_2CH); 25.44 (*q*, Me); 23.06 (*q*, Me); 22.46, 22.30 (2*q*, Me_2CH). GC/MS ($C_{20}H_{21}NO_2$; 307.39): 307.1 (100, $M^{+\cdot}$), 292.1 (35, $[M - Me]^+$), 276.1 (29, $[M - MeO]^+$), 256.1 (19, $[M - HC{\equiv}CCN]^{+\cdot}$), 248.1 (24, $[M - MeOCO]^+$), 198.1 (67, $[M - MeOCOC{\equiv}CCN]^{+\cdot}$).

1.2. *Methyl (*E*)-3-[9-Isopropyl-5-(methoxycarbonyl)-1,6-dimethylheptalen-4-yl)prop-2-enoate* (**12**). Formyl-ester **10** (0.025 g, 0.80 mmol) [1][7] was dissolved in benzene (3 ml). The soln. was stirred with Al_2O_3 (0.90 g) during 5 min. The solvent was evaporated, and again benzene (10 ml) was added, followed by [(methoxycarbonyl)methylidene](triphenyl)-λ^5-phosphane (0.36 g, 1.07 mmol) (*Fluka*). The mixture was stirred during 8 h. The solvent was distilled off, and the residue was subjected to CC (silica gel; hexane/Et_2O 1:2) to give pure **12** (0.11 g, 37%), which exists in solution at r.t. as a thermal 2:1 equilibrium mixture with its DBS isomer **12′**. M.p. 147° (hexane/Et_2O). R_f (hexane/Et_2O 1:2) 0.35/0.26. UV (MeCN): λ_{max} 298.5 (4.38). ^1H-NMR 600 MHz, C_6D_6; 2:1 mixture **12**/**12′**): signals of **12**: 7.586 (*d*, $^3J = 16.0$, H–C(3)); 6.298 (*d*, $^3J = 6.2$, H–C(3′)); 6.166 (*d*, $^3J = 6.4$, H–C(8′)); 6.100 (*d*, $^3J = 16.0$, H–C(2)); 6.035 (*dq*-like, $^3J = 6.4$, $^4J = 1.2$, H–C(7′)); 5.778 (*s*, H–C(10′)); 5.761 (*dq*-like, $^3J = 6.5$, $^4J = 1.3$, H–C(2′)); 3.366 (*s*, MeOCO–C(5′)); 3.356 (*s*, MeOC(1)O–C(2)); 2.253 (*sept.*, $J = 6.9$, Me_2CH); 1.962 (*s*, Me–C(6′)); 1.783 (*s*, Me–C(1′)); 0.930/0.913 (2*d*, $J = 6.9$, 6.8, Me_2CH). ^{13}C-NMR (150 MHz, C_6D_6; 2:1 mixture **12**/**12′**): signals of **12**: 168.35 (MeO*C*O–C(5′)); 166.97 (MeO*C*(1)O–C(2)); 148.58 (C(9′)); 147.42 (C(3)); 143.92 (C(5′a)); 142.15 (C(1′)); 138.37 (C(3′)); 138.24 (C(4′)); 133.07 (C(10′a)); 128.45 (C(6′)); 127.80 (C(7′)); 126.75 (C(2′)); 125.69 (C(10′)); 125.63 (C(8′)); 124.53 (C(5′)); 118.03 (C(2)); 51.67 (*Me*OCO–C(5′)); 50.96 (*Me*OCO–C(2)); 35.85 (Me_2CH); 25.08 (*Me*–C(1′)); 22.31 (*Me*–C(6′)); 23.02, 22.52 (Me_2CH). ^1H-NMR (600 MHz, C_6D_6; 2:1 mixture **12**/**12′**): signals of **12′**: 8.872 (*d*, $^3J = 16.0$, H–C(3)); 6.447 (*d*, $J = 11.8$, H–C(3′)); 6.263 (*d*, $J = 16.0$, H–C(2)); 6.256 (*d*, $^3J = 11.9$, H–C(4′)); 6.246 (*d*, $^3J = 11.9$, H–C(9′)); 6.212 (*dd*-like, $^3J = 11.9$, $^4J = 1$, H–C(8′)); 5.755 (*s*, H–C(6′)); 3.417 (*s*, MeOCO–C(1′)); 3.297 (*s*, MeOC(1)O–C(2)); 2.362 (*sept.*, $J = 7.0$, Me_2CH); 1.655 (*s*, Me–C(10′)); 1.574 (*s*, Me–C(5′)); 1.036/1.023 (2*d*, $J = 7$, Me_2CH). ^{13}C-NMR (150 MHz, C_6D_6; 2:1 mixture **12**/**12′**): signals of **12′**: 166.67 (MeO*C*(1)O–C(2)); 166.65 (MeO*C*O–C(1′)); 148.24 (C(7′)); 141.95 (C(3)); 141.40 (C(2′)); 138.98 (C(4′)); 137.05 (C(5a)); 136.03 (C(9′)); 132.79 (C(10′a)); 131.81 (C(8′)); 130.46 (C(10′)); 129.89 (C(5′)); 127.33 (C(3′)); 123.36 (C(2)); 122.26 (C(6′)); 51.68 (*Me*OC(1)O–C(2)); 51.26 (*Me*OCO–C(1′)); 34.99 (Me_2CH); 22.97,

22.74 (*Me*$_2$CH); 17.69 (*Me*–C(10′)); 16.70 (*Me*–C(5′)). EI-MS ($C_{23}H_{26}O_4$; 366.45): 366.1 (25, $M^{+\cdot}$), 351.1 (5, $[M-Me]^+$), 307.1 (4, $[M-MeOCO]^+$), 256.1 (6, $[M-HC{\equiv}C-CH{=}CHCOOMe]^{+\cdot}$), 198 (100, $[M-MeOCOC{\equiv}C-CH{=}CHCOOMe]^{+\cdot}$), 183.1 (32, $[M-(Me+MeOCOC{\equiv}C-CH{=}CHCOOMe)]^+$), 84.0 (92, $[HC{\equiv}CCOOMe]^{+\cdot}$).

1.3. *Formation of the 1-[(*E*)-2-(Dialkylamino)ethenyl]-Substituted Heptalene-5-carboxylates* **8a**–**8k** (*cf. Table 1*). 1.3.1. *General Procedure for* **8b**–**8i**. A soln. of the cyclic amine (5 mmol) and of *N,N*-dimethylformamide dimethyl acetal (DMFDMA, 5 mmol; *Fluka*) in DMF (5 ml) was stirred during 1 h at 100°. After cooling to 50°, a soln. of the corresponding heptalenes (1 mmol) in DMF (5 ml) was added. The mixture was stirred at 50–110° during 1–6 h until all starting heptalene had been consumed. DMF was distilled off and the residue purified by CC (silica gel; hexane/Et_2O 2:1). The new heptalenes **8b**–**8i** were characterized by their UV/VIS spectra (see *Tables 7* and *8* as well as *Figs. 4–7*), ^{1}H- and ^{13}C-NMR spectra (see *Tables 3–5*), and, partially, by their IR spectra (see *Table 6* and *Fig. 3*). M.p. and R_f (hexane/Et_2O 1:2) values: **8b** 102.5°/0.17; **8c** 157.0°/0.18; **8d** 109.8°/0.45; **8e** 92.8°/0.35; **8f** 150.7°/0.51; **8g** 87.0°/0.45; **8h** 99.1°/0.34(0.50); **8i** 180.1°/0.21.

The heptalene-4,5-dicarboxylates **8c** and **8i** were also subjected to X-ray crystal-structure analyses (see *Tables 2* and *10*, and *Fig. 2* as well as *Sect. 2*).

1.3.2. *General Procedure* for **8a** and **8k**: It was the same as described under 1.3.1 with the exception that no preceding transamination reaction was necessary. M.p. and R_f (hexane/Et_2O 1:2) values: **8a** 91.2°/0.24; **8k** 132.3°/0.51.

1.4. *Irradiation Experiments.* 1.4.1. *Formation of Dimethyl 5-[(*E*)-2-Pyrrolidinoethenyl]-6,8,10-trimethylheptalene-1,2-dicarboxylate* (**8′i**). Heptalene **8i** was irradiated in C_6D_6 ($c \approx 1 \cdot 10^{-5}$ M) with a W lamp until a photostationary state between **8i** and **8′i** (*ca.* 15:85) was established. UV/VIS: *Table 8* and *Fig. 10*. ^{1}H-NMR: *Table 3*.

Irradiation of **8i** ($c \approx 1 \cdot 10^{-5}$ M) in hexane or MeCN in a UV/VIS cuvette with a W lamp led again rapidly to a photostationary state of **8i** and **8′i** (*cf. Fig. 8*). Heating the mixture in the cuvette at >40° established the UV/VIS spectrum of pure **8i**.

1.5. *Formation of Dimethyl 1-(Formylmethyl)-9-isopropyl-6-methylheptalene-4,5-dicarboxylate* (**13**). Heptalene **8a** (0.050 g, 0.126 mmol) was dissolved in a mixture of THF (3 ml) and H_2O (0.5 ml), followed by addition of a catal. amount of AcOH (1 drop). The mixture was stirred during 5 h at r.t. Et_2O was added. The org. phase was washed 3 times with H_2O and then dried ($MgSO_4$). The solvent was removed, and the residue was filtered through a short column (silica gel; hexane/Et_2O 1:1) to give pure **13** as a pale yellow, semicrystalline solid (0.046 g, 99%), which was not very stable. IR ($CHCl_3$/KBr): 1725/1722*s* (CHO). ^{1}H-NMR (300 MHz, C_6D_6): 9.09 (*t*, ^3J = 1.8, –CHO); 7.51 (*dd*, ^3J = 6.2, ^5J = 1.2, H–C(3)); 6.12 (*dd*, ^3J = 6.6, ^4J = 0.9, H–C(8)); 6.01 (*dq*-like, ^3J = 6.6, ^4J = 1.4, H–C(7)); 5.65 (*s*, H–C(10)); 5.61 (*d*, ^3J = 6.2, H–C(2)); 3.43 (*s*, MeOCO–C(5)); 3.29 (*s*, MeOCO–C(4)); 2.87 (*A* of *AB*, *dq*, J_{AB} = 16.2, $\Sigma\,^3J$ = 4.7, CH_2–C(1)); 2.65 (*B* of *AB*, *dd*, J_{AB} = 16.6, ^4J = 1.7, CH_2–C(1)); 2.22 (*sept.*, *J* = 6.8, Me_2CH); 2.13 (*s*, Me–C(6)); 0.91, 0.90 (2*d*, *J* = 6.9, 6.8, *Me*$_2$CH). ^{13}C-NMR (75 MHz, C_6D_6): 195.90 (*d*, CHO); 167.44 (*s*, MeO*C*O–C(5)); 167.07 (*s*, MeO*C*O–C(4)); 148.12 (*s*, C(9)); 144.82 (*s*, C(5a)); 138.78 (*d*, C(3)); 137.71 (*s*, C(1)); 134.92 (*s*, C(10a)); 130.76 (*s*, C(4)); 130.03 (*s*, C(6)); 129.49 (*d*, C(2)); 127.97 (*d*, C(7)); 127.34 (*d*, C(10)); 126.47 (*d*, C(8)); 124.77 (*s*, C(5)); 53.23 (*t*, CH_2); 51.63 (*q*, *Me*OCO–C(4)); 51.58 (*q*, *Me*OCO–C(5)); 35.70 (*d*, Me_2CH–C(9)); 22.97, 22.43 (*q*, *Me*$_2$CH–C(9)); 22.92 (*q*, *Me*–C(6)).

2. X-Ray Crystal-Structure Determinations of 8c and 8i[4]). – 2.1. The structure of **8c** ($C_{26}H_{31}NO_4$) has been solved and refined successfully (*cf. Fig. 2,a*, and *Tables 2* and *10*). The crystal used was quite weakly diffracting. As a result, there is a paucity of observed reflections, which leads to slightly less accurate structural parameters than normal. However, the structure is clearly defined. Enlarged atomic displacement ellipsoids for i-Pr–C(9) suggest that there may be slight disorder in this group, but a disordered model could not be developed adequately.

2.2. The structure of **8i** ($C_{25}H_{29}NO_4$) has been solved and refined successfully with no unusual features (*cf. Fig. 2,b*, and *Tables 2* and *10*).

---

[4]) Crystallographic data (excluding structure factors) for the structures reported in this paper have been deposited with the *Cambridge Crystallographic Data Center* as supplementary publication nos. CCDC-162360 and 162361 for **8c** and **8i**, resp. Copies of the data can be obtained, free of charge, on application to the CCDC, 12 Union Road, Cambridge CB21EZ, UK (fax: +44-(0)1223-336033; email: deposit@ccdc.cam.ac.uk).

Table 10. *Crystallographic Data of Heptalene-4,5-dicarboxylates* **8c** *and* **8i**

	8c	**8i**
Crystallized from	AcOEt/pentane	AcOEt/pentane
Empirical formula	$C_{26}H_{31}NO_4$	$C_{25}H_{29}NO_4$
Formula weight [g·mol^{-1}]	421.53	407.51
Crystal color, habit	red, tablet	red, prism
Crystal dimensions [mm]	$0.22 \times 0.40 \times 0.50$	$0.24 \times 0.36 \times 0.48$
Temp. [K]	295(1)	295(1)
Crystal system	monoclinic	triclinic
Space group	$P2_1/n$	$P\bar{1}$
Z	4	2
Reflections for cell determination	25	25
2θ Range for cell determination [°]	22 – 38	35 – 40
Unit-cell parameters		
a [Å]	10.884(2)	11.584(1)
b [Å]	14.721(2)	13.852(1)
c [Å]	15.120(2)	7.287(1)
α [°]	90	97.40(1)
β [°]	99.27(1)	100.60(1)
γ [°]	90	97.641(7)
V [Å^3]	2390.8(6)	1124.9(3)
$F(000)$	904	436
D_x [g cm^{-3}]	1.171	1.203
$\mu(\mathrm{Mo}K_\alpha)$ [mm^{-1}]	0.0782	0.0808
Scan type	$\omega/2\theta$	$\omega/2\theta$
$2\theta_{(\max)}$ [°]	55	55
Total reflections measured	5985	5419
Symmetry-independent reflections	5471	5162
R_{int}	0.045	0.010
Reflections used [$I > 2\sigma(I)$]	1953	3472
Parameters refined	281	272
Reflection/parameter ratio	6.95	12.8
Final R	0.0607	0.0493
wR	0.0414	0.0459
Weights: p in $w = [\sigma^2(F_o) + (pF_o)^2]^{-1}$	0.005	0.005
Goodness-of-fit	1.768	2.337
Secondary extinction coefficient	$2.6\ (6) \times 10^{-7}$	$1.8\ (2) \times 10^{-6}$
Final $\Delta_{\max}/\sigma$	0.0002	0.0004
$\Delta\rho$ (max; min) [e Å^{-3}]	0.24; −0.22	0.17; −0.17
$\sigma(d(\mathrm{C-C}))$ [Å]	0.005 – 0.007	0.002 – 0.003

REFERENCES

[1] a) A. A. S. Briquet, P. Uebelhart, H.-J. Hansen, *Helv. Chim. Acta* **1996**, *79*, 2282; b) S. El Houar-Maillefer, H.-J. Hansen, *Helv. Chim. Acta* **1997**, *80*, 253; c) S. El Houar-Maillefer, Ph. D. Thesis, University of Zurich, 1998.

[2] H. Meerwein, F. Werner, N. Schön, G. Stopp, *Liebigs Ann. Chem.* **1961**, *641*, 1.

[3] H. Bredereck, F. Effenberger, H. Botsch, *Chem. Ber.* **1964**, *97*, 3397; H. Bedereck, G. Simchen, R. Wahl, *Chem. Ber.* **1968**, *101*, 4048.

[4] W. Leimgruber, A. D. Batcho, Third International Congress of Heterocyclic Chemistry, Tohoku University, Sendei, Japan, 1971; U.S. Patent 3732245, 1973.

[5] R. D. Clark, D. B. Repke, *Heterocycles* **1984**, *22*, 195.

[6] J. Song, H.-J. Hansen, *Helv. Chim. Acta* **1999**, *82*, 2260.

[7] J. Guspanová, R. Knecht, M. Laganà, C. Weymuth, H.-J. Hansen, *Helv. Chim. Acta* **1997**, *80*, 1375.

[8] P. Uebelhart, H.-J. Hansen, *Helv. Chim. Acta* **1992**, *75*, 2493.
[9] K. Hafner, G. L. Knaup, H. J. Lindner, *Bull. Chem. Soc. Jpn*. **1988**, *61*, 155.
[10] W. Bernhard, P. Brügger, J. J. Daly, G. Englert, P. Schönholzer, H.-J. Hansen, *Helv. Chim. Acta* **1985**, *68*, 1010.
[11] G. Häfelinger, H.-G. Mack, in 'The Chemistry of Enamines', Ed. Z. Rappoport, John Wiley & Sons Ltd., Chichester, 1994, p. 1.
[12] P. Kouroupis, H.-J. Hansen, *Helv. Chim. Acta* **1995**, *78*, 1247.
[13] P. Uebelhart, P. Mohler, R.-A. Fallahpour, H.-J. Hansen, *Helv. Chim. Acta* **1995**, *78*, 1437.
[14] W. Bernhard, P. Brügger, J. J. Daly, P. Schönholzer, R. H. Weber, H.-J. Hansen, *Helv. Chim. Acta* **1985**, *68*, 415.
[15] G. Opitz, W. Merz, *Liebigs Ann. Chem*. **1962**, *652*, 139; N. F. Firrell, P. W. Hickmott, B. J. Hopkins, *J. Chem. Soc. (B)* **1971**, 351.
[16] T. Shono, in 'The Chemistry of Enamines', Ed. Z. Rappoport, John Wiley & Sons Ltd., Chichester, 1994, p. 459.
[17] G. Bourhill, J.-L. Brédas, L.-T. Cheng, S. R. Marder, F. Meyers, J. W. Perry, B. G. Tiemann, *J. Am. Chem. Soc*. **1994**, *116*, 2619.
[18] T. Landmesser, H.-J. Hansen, unpublished results.
[19] M. J. Kamlet, E. G. Kayser, J. W. Eastes, W. H. Gilligan, *J. Am. Chem. Soc*. **1973**, *95*, 5210.
[20] D. J. Cowley, *J. Chem. Soc., Perkin Trans. II*, **1975**, 287; V. Bekárek, V. Bekárek Jr., *Coll. Czech. Chem. Comm*. **1987**, *52*, 287.
[21] O. W. Kolling, *Anal. Chem*. **1981**, *53*, 54.
[22] C. Reichardt, 'Solvents and Solvent Effects in Organic Chemistry', VCH, Weinheim, 1988.
[23] G. Buemi, F. Zuccarello, *Gazz. Chim. Ital.* **1985**, *115*, 103.
[24] G. Rüedi, H.-J. Hansen, *Helv. Chim. Acta* **2001**, *84*, 1017.

Received May 25, 2001